Tribol Lett (2011) 44:99–106
DOI 10.1007/s11249-011-9832-4

METHODS PAPER

Near-Edge X-ray Absorption Fine Structure Imaging of Spherical and Flat Counterfaces of Ultrananocrystalline Diamond Tribological Contacts: A Correlation of Surface Chemistry and Friction

A. R. Konicek · C. Jaye · M. A. Hamilton · W. G. Sawyer · D. A. Fischer · R. W. Carpick

Received: 30 September 2010 / Accepted: 21 July 2011 / Published online: 13 August 2011

Abstract A recently installed synchrotron radiation near-edge X-ray absorption fine structure (NEXAFS) full field imaging electron spectrometer was used to spatially resolve the chemical changes of both counterfaces from an ultrananocrystalline diamond (UNCD) tribological contact. A silicon flat and Si_3N_4 sphere were both coated with UNCD, and employed to form two wear tracks on the flat in a linear reciprocating tribometer. The first wear track was produced using a new, unconditioned sphere whose surface was thus conditioned during this first experiment. This led to faster run-in and lower friction when producing a second wear track using the conditioned sphere. The large depth of field of the magnetically guided NEXAFS imaging detector enabled rapid, large area spectromicroscopic imaging of both the spherical and flat surfaces. Laterally resolved NEXAFS data from the tribological contact area revealed that both substrates had an as-grown surface layer that contained a higher fraction of sp^2-bonded carbon and oxygen which was mechanically removed. Unlike the flat, the film on the sphere showed evidence of having graphitic character, both before and after sliding. These results show that the graphitic character of the sphere is not solely responsible for low friction and short run-in. Rather, conditioning the sphere, likely by removing asperities and passivating dangling bonds, leads to lower friction with less chemical modification of the substrate in subsequent tests. The new NEXAFS imaging spectroscopy detector enabled a more complete understanding of the tribological phenomena by imaging, for the first time, the surface chemistry of the spherical counterface which had been in continual contact during wear track formation.

Keywords Friction mechanisms · Solid lubrication friction · Spectroscopy · Humidity · Diamond · Carbon · Solid lubrication mechanisms · Solid lubrication wear · Coatings · NEXAFS

A. R. Konicek (✉)
Physics & Astronomy Department, University of Pennsylvania, Philadelphia, PA 19104, USA
e-mail: andy.konicek@gmail.com

Present Address:
A. R. Konicek
National Institute of Standards and Technology (NIST), Gaithersburg, MD 20899, USA

C. Jaye · D. A. Fischer
Material Measurement Laboratory, National Institute of Standards and Technology, Gaithersburg, MD 20899, USA

M. A. Hamilton · R. W. Carpick
Department of Mechanical Engineering and Applied Mechanics, University of Pennsylvania, Philadelphia, PA 19104, USA

Present Address:
M. A. Hamilton
Exactech, Inc, Gainesville, FL 32653, USA

W. G. Sawyer
Mechanical and Aerospace Engineering Department, University of Florida, Gainesville, FL 32611, USA

1 Introduction

In the search for better understanding of tribological phenomenon, there is a drive to employ new tools and techniques to better characterize the contacting, sliding interfaces. More complete knowledge of the mechanical, structural, and chemical properties of surfaces and interfaces will yield insight into new, phenomenological behaviors. Local characterization of chemical information

is a critical component, leading to new theories and predictive capabilities for the friction and wear of materials.

Such information is particularly important to study in the case of high performance tribological materials to understand the factors that contribute to low friction and wear. Ultrananocrystalline diamond (UNCD), due to its high modulus and hardness [1, 2] combined with low friction and wear [3, 4], is an exceptional tribological material. Able to be coated in thin film form, UNCD has ~2–5 nm diameter equiaxed diamond grains with ~0.5 nm grain boundaries [5], resulting in a film with as high as 98% sp^3-bonded carbon [6, 7]. The small grain size, which does not change with film thickness, also means it is one of the smoothest diamond films available, with an RMS roughness of <12 nm over a 1 × 1 μm^2 area [6]. However, UNCD suffers from an environmental dependence. In ambient or humidified environments the friction and wear are low, but in inert or vacuum environments the friction and wear both increase by an order of magnitude or more [3, 8].

Previous studies have examined the tribological properties of novel, hydrogen-free carbon films, such as hydrogen-free diamond-like carbon (H-free DLC), nanocrystalline diamond (NCD), and UNCD. Eryilmaz et al. [9] measured the friction behavior of H-free DLC with and without treatment in a hydrogen plasma. Testing the untreated film in a N_2 environment, the friction coefficient rose to 0.88 within a meter of sliding and then settled down to around 0.1. The coating on the sphere completely wore through, and this test was stopped after 12 m of total travel. After treatment of the as-grown DLC with a hydrogen plasma, the friction coefficient quickly reached 0.1, but went down to 0.015 after 10 m of sliding. By contrast, this test lasted for 470 m of total travel, and the final friction coefficient was ~0.008. The worn and unworn areas were characterized using imaging time-of-flight secondary ion mass spectrometry (TOF-SIMS). TOF-SIMS uses an ion source to sputter away material while simultaneously measuring the mass and starting position of the fragmented pieces. 3-D data was obtained, with slices ~1 nm thick and 500 × 500 μm^2 laterally, of the chemical composition of the sample surface before and after H-plasma treatment. They found that the post-H-plasma surface had increased fractions of H and CH species, and diminished carbon (C_1, C_2, and C_4) fractions. Improved friction properties are believed to be caused by hydrogen passivating dangling σ-bonds at the surface, reducing adhesive interactions across the interface. While TOF–SIMS gives excellent compositional and spatial information, it tells nothing about the bonding types present. On top of being a destructive technique, it is also possible that the ion sputtering alters the sub-surface layer composition, and further confuses the information from the specific fragment species.

The run-in behavior of NCD was examined by Chromik et al. [10] using an in situ tribometer. Several NCD films were grown, by varying the source gas H_2 content, in an effort to have films with a range of nanostructures. These films were then characterized by a battery of surface morphology (atomic force and scanning electron microscopies) and chemistry techniques (Near-edge X-ray absorption fine structure, NEXAFS and Raman spectroscopies). Reciprocating tribometry was performed using a 6.35 mm diameter sapphire pin, with a 6.4 N load, sliding against the various films in air at 35–45% relative humidity (RH). The in situ tribometry setup allows for optical measurements that can observe wear, through debris formation and removal, and resolve velocity accommodation modes, thereby explaining the lubrication process. They found that films with a higher H_2 source gas concentration had fewer run-in cycles and experienced less wear. X-ray diffraction analysis and NEXAFS spectroscopy showed that these films also contained more sp^2-bonded carbon that had graphite-like order. This decrease in run-in cycles was in spite of the films being rougher. Sapphire was used to perform the in situ tribometry measurements since the counterface must be optically transparent. This complicates the interpretation by introducing a material that is not as mechanically robust as NCD, and introduces Al and O into the tribochemistry, since the sapphire ball wears against the harder NCD and thus deposits inside the wear track. It would be difficult to accurately represent a situation of NCD-on-NCD friction, such as might be seen in an actual device. Raman spectroscopy was taken on the flats and spheres before and after the tribometry. Pre-test measurements on the flat showed that the signals were different for the films grown with the lowest and highest H_2 fractions, but the others were almost identical. Raman data from the post-test spheres revealed the presence of a transfer film that was largely indistinguishable from the unworn material, showing the sapphire peak and a broadening of the same NCD features. NEXAFS spectroscopy, a non-spatially-resolved technique that is more sensitive to carbon bonding states, was performed as a bulk characterization technique on the as-grown samples, but no laterally resolved data were collected from the worn areas to examine how the chemistry had changed due to wear.

As was mentioned, tribochemical changes that occur in carbon films are well characterized by NEXAFS. NEXAFS probes the density of unoccupied electronic states, which is very sensitive to local bonding chemistry (C, H, and O) as well as bonding type (single-, double-bonded). Photoelectron emission microscopy (PEEM) is an electron imaging method that can be combined with NEXAFS to study tribological systems [11–13], and has been used to study UNCD [3, 14]. The sample is held at a large (around −15 kV) negative bias so that the emitted photoelectrons

leave the surface in a perpendicular trajectory. However, this prevents measurement of non-planar surfaces, meaning the counterfaces in tribological contacts, usually spherical, cannot be characterized.

Here we discuss the use of a new spatially-resolved spectroscopy tool, a large area rapid imaging analytical tool (LARIAT) www.synchres.com (schematic and picture shown in Fig. 1). This synchrotron-based system utilizes NEXAFS spectroscopy, collected in a partial electron yield mode, while magnetically guiding the emitted electrons to form an image of the NEXAFS signal over a $\sim 13 \times 18$ mm^2 region. Unlike PEEM, the new spectroscopic imaging technique at the National Synchrotron Light Source (NSLS) can handle samples of a non-planar geometry. This makes this technique very attractive for the *ex situ* characterization of tribological contacts with both flat and spherical counterfaces.

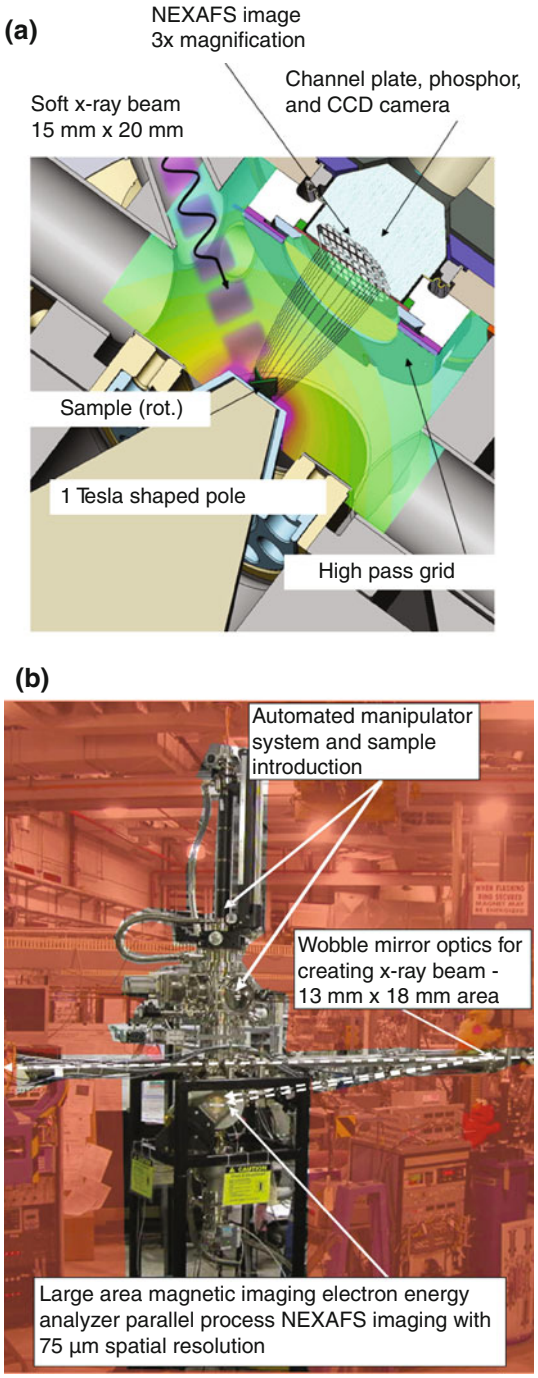

Fig. 1 **a** Schematic of the inside of the imaging chamber. **b** Photograph of the imaging endstation *(background shaded)*.

2 Experiment

The imaging NEXAFS measurements were performed using the parallel processing imaging system at NIST beamline U7A (Fig. 1), located at the NSLS. The imaging soft X-ray beam rastered across a full field area of 18×13 mm^2 on the sample. The technique combines NEXAFS spectroscopy, full field parallel process magnetic field electron yield optics detector, and a large incident soft X-ray beam on the sample. The rapid parallel processing magnetic field electron yield optics detector produced a series of two-dimensional NEXAFS lateral images as the incident soft X-ray energy was scanned above the *K* absorption edges. The image stack reveals information about the bond chemistry at the surface with 50 µm planar spatial resolution. Electron emission spectra were acquired using a photon energy range of 270–340 eV around the carbon *K*-edge, and 515–570 eV around the oxygen *K*-edge, with energy resolutions of approximately 0.1 and 0.2 eV, respectively. To eliminate the effect of incident beam intensity fluctuations and absorption features in the beamline optics, the PEY signals were normalized by the photo yield of a clean gold mesh located upstream along the path of the incident X-ray beam.

To produce the wear tracks, silicon flats (1×1 cm^2) and Si_3N_4 spheres (3 mm diameter) were coated with UNCD by microwave plasma chemical vapor deposition in a DiamoTek 1800 series 915 MHz, 10 kW MPCVD system installed at Argonne National Laboratory [15]. The growth temperature was 650 °C, which is lower than the growth temperature for typical UNCD [6]. Films were grown on the flats and the spheres at the same time to a thickness of ~ 1 µm. The Si_3N_4 spheres had a flat spot polished on them that was positioned away from the growth source. They were mounted using this polished spot for all subsequent tests so that identifying the same analysis region is consistent.

Tribometry tests were carried out using a microtribometer housed in a sealed chamber to control the RH in the test environment, described in more detail elsewhere [16], and used for other diamond tribology experiments [3, 14]. The wear tracks were created in a bidirectional linear reciprocation mode. Carbon films undergo a period of higher friction

and higher wear as sliding begins, called run-in, where surface asperities are worn away. The higher the initial roughness, the longer the period of run-in [17]. To condition the sphere, the first test (referred to as Track #1) consisted of sliding for 5000 cycles. Then the same contact point of the sphere was positioned over a new part of the flat sample and a second wear track (referred to as Track #2) was run for 3000 cycles. Both tracks were created in a 5.0% RH with N_2 environment, with a 1.0 N load (initial mean Hertzian contact stress of 649 MPa), a 1.0 mm/s sliding speed, and a 500 μm track length. The goal was to determine the surface chemical state of the sphere and flat, and the steady-state friction value, after running in the sphere. Friction values as a function of position along the track were calculated by taking the measured point-wise friction force and dividing by the normal force. Friction coefficients per cycle are calculated by averaging the positional friction data from the middle 70% of the track.

To characterize the UNCD wear, scanning white light profilometry measurements were performed on the tracks using a Zygo NewView 6300 interferometer. A height profile was taken on each track with lateral resolution of ~0.5 μm and vertical resolution at 0.1 nm. For a wear track that is 500 μm long and 50 μm wide, and assuming the uncertainty in the height of every pixel is 10 nm, there would be an uncertainty in the measured wear volume of 2.7×10^{-7} mm^3. In the worst case, using a load of 1.0 N, 3,000 cycles, and a 500 μm track length, the uncertainty in the wear rate would be greater than 5.0×10^{-8} mm^3 N^{-1} m^{-1}.

3 Results

The friction data for the two wear tracks are shown in Fig. 2. Track #1 (Fig. 2, black) friction data starts off at 0.244 ± 0.005 for ~1,200 cycles, and then the sphere and track run in after 3,000 cycles to a friction coefficient of 0.0371 ± 0.0008. When the test was stopped after 5,000 cycles, the friction coefficient had reached a steady-state value of 0.0337 ± 0.0003. The friction measurements for Track #2 (Fig. 2, gray) underwent a run-in to a friction coefficient of 0.04 in <40 cycles, and eventually hit a minimum of 0.0215 ± 0.0002 at 191 cycles. The friction coefficient slowly increases for the remaining cycles of the test and is at 0.028 ± 0.001 at cycle 3,000.

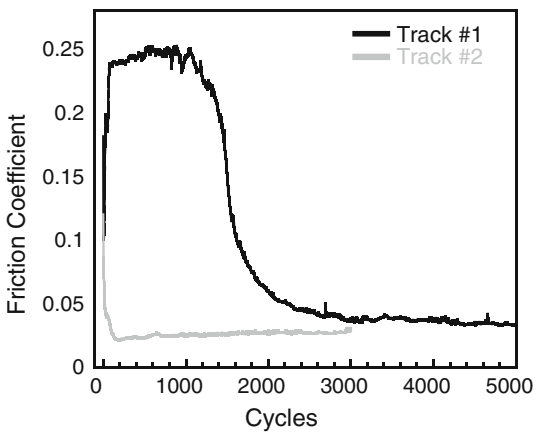

Fig. 2 Friction data from Track #1 *(black line)* and for Track #2 *(gray line)* made in a new location on the sample.

The profilometry results show that the two tracks have a different height profile. In both cases, the wear of the track is low overall. Track #1 had a maximum depth of ~43 nm inside the gouge, and a single-point wear rate of 3.2×10^{-8} mm^3 N^{-1} m^{-1}. The single-point wear rate is calculated from measurements of the initial and final topography of the wear track, and assumes the wear progression is linear. Since UNCD has such low roughness, the initial state of the film is assumed to be flat. Though the worn region for Track #2 could be identified in the profilometer, the track height profile was not distinguishable from the surface roughness of the film. As such, the measured wear volume (and therefore the calculated wear rate) was below the uncertainty of the system.

The NEXAFS images for the sphere and flat include the areas modified by wear as well as areas of unworn material. Fig. 3a is a full field electron image at 289.0 eV of the UNCD flat. The bright stripes are regions that were coated with 40 nm of platinum for a separate study. The dark upper and upper right regions reflect the limits of the illumination of the X-rays. Four tracks are visible in the image. The carbon NEXAFS data (Fig. 3b) are from the two tracks in this study (ROIs labeled in Fig. 3a) and an unworn region (not drawn in Fig. 3a). These spectra have a peak at 285.0 eV that is due to the disordered carbon–carbon double bonds [18]. An exciton at ~289.3 eV and the second band gap at ~302 eV are typical diamond features. The peak at 286.6 eV is from C=O bonding. There is a slight feature in both tracks at 287.5 from C–H bonds. Both Tracks #1 and #2 have higher C=C concentrations than the unworn area, with Track #1 having more. Track #1 also has the higher amount of C=O bonding, whereas Track #2 actually has less than the unworn area. Figure 3c has O 1 s NEXAFS spectra from the same regions from which the C 1 s spectra in Fig. 3b were taken. All spectra have the same intensity peak at ~533.0 eV from the O=C bonds. There is also a feature at ~535.5 eV that is higher in the unworn spectrum than for both Tracks #1 and #2.

Figure 4a is an image (taken at 289.0 eV) of the UNCD coated sphere employed to make the two tracks highlighted in Fig. 3a (image at 289.0 eV). Carbon NEXAFS data (Fig. 4b) were taken from the worn region on the sphere as

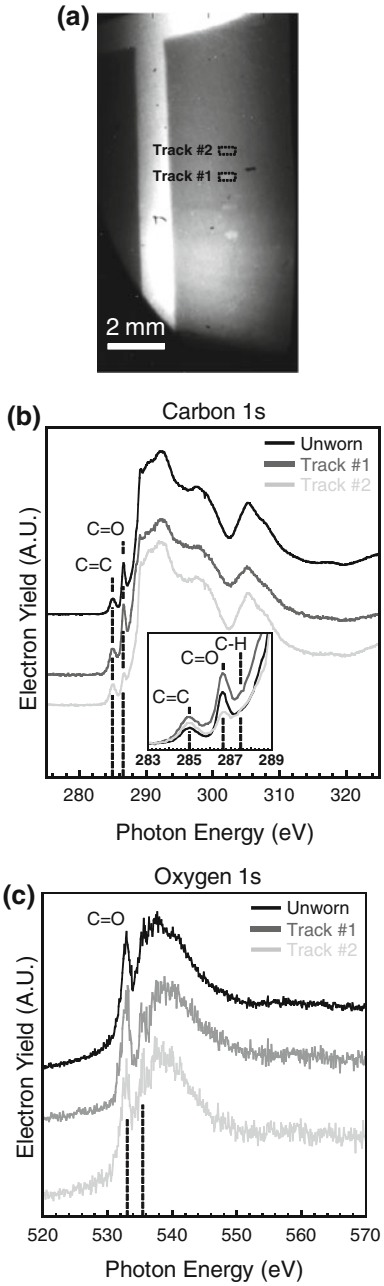

Fig. 3 **a** NEXAFS image of UNCD coated silicon flat. **b** Carbon NEXAFS spectra from unworn area *(black)*, Track #1 *(dark gray)*, and Track #2 *(light gray)*. **c** Oxygen NEXAFS spectra from same regions.

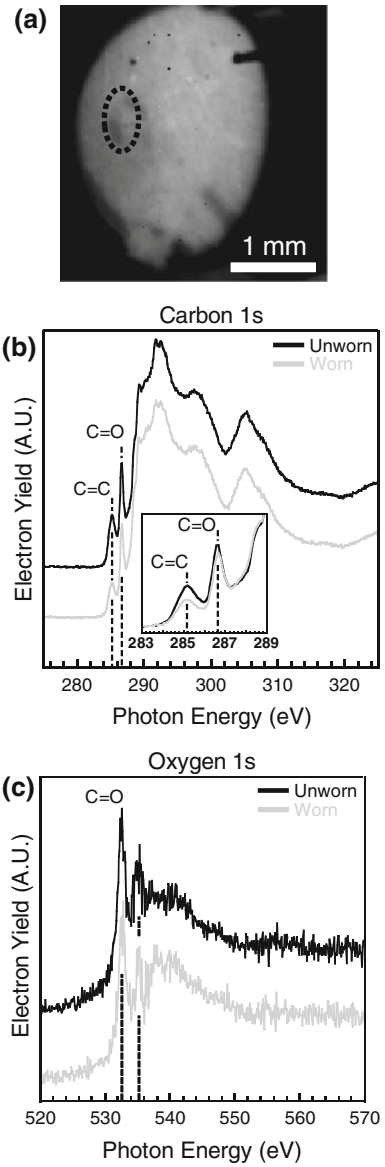

Fig. 4 **a** NEXAFS image of UNCD coated Si_3N_4 sphere. **b** Carbon NEXAFS spectra from unworn area *(black)* and worn area *(gray)*. **c** Oxygen NEXAFS spectra from same regions.

well as the unworn film. The worn region of interest (ROI) is drawn in Fig. 4a. Both spectra have a peak at 285.2 eV, that is from a combination of the presence of disordered [18] and ordered [19, 20] carbon–carbon double bonds. There is an edge jump with an excitonic feature at ~289.3 eV and a dip in intensity at ~302 eV. These features are common to materials with a high fraction of ordered sp^3-bonded carbon, i.e., diamond [21]. There is also a feature at ~286.7 eV from C=O bonds [22, 23]. The double peak around 292.0 eV is more intense than typical UNCD spectra, and looks like the σ^* post-edge features from a highly oriented pyrolitic graphite (HOPG) spectrum [20]. The only noticeable differences between the two spectra are the peak heights at ~285.2 and ~286.6 eV. The unworn film has more sp^2-bonded carbon as well as more C=O bonds than the worn region (inset of Fig. 4b). The oxygen spectra (Fig. 4c) show differences in the level of oxidation. The unworn spectrum has higher peaks at both ~532.6 and ~535.4 eV, which are π^* features of O=C bonding [24].

4 Discussion

One of the open questions of only studying the chemical changes on the flat from a pin-on-flat tribometer geometry is that it is possible that the pin is not changing in the same manner as the flat. The pin is in constant contact with the flat during sliding, while portions of the flat are fully exposed to the environment during for part of the sliding cycle. This means portions of the track have a longer exposure time to interact with the environment. The chemical passivation of the flat might then have a very different final state than that of the pin. The pin also experiences the longest time in contact with the counterface (100%), whereas the rest of the track is only a fraction of that (depending on track length and contact area).

These results show that the tribological behavior of this self-mated UNCD contact is dependent on the initial condition of the sphere's surface (*i.e.*, roughness and chemistry). Track #1 experiences a longer period of high friction and has a high wear rate, compared with Track #2. NEXAFS data for Track #1 (Fig. 3b, c) show that it had more amorphous carbon, C=O bonds, and C–H bonds than the unworn film. There is no shift in the C=C peak that would indicate ordered bonding, or graphitization. This shows that the period of high friction broke the carbon bonds, and those bonds amorphously rehybridized or bonded to species in the environment, most likely water. The increase in amorphous carbon is also evident by the reduction in the depth of the second band gap feature whose minimum is at 302.0 eV, which is caused by the increased fraction of carbon–carbon species with a range of non-diamond bond lengths or orientations.

In contrast, Track #2 ran in immediately, and has a much lower wear rate. The C 1s NEXAFS data show that Track #2 has a nearly identical C=C peak to the unworn spectrum, only slightly higher, suggesting some additional amorphous carbon has been formed or deposited on the surface. The largest difference is from 286–289 eV. The C=O peak at $\sim$286.6 eV for Track #2 is lower than that in either the unworn or the Track #1 spectrum. The C–H peak has the same intensity as the unworn spectrum. The lack of O– and H– bonding signifies that the surface underwent little bond breaking and reconstruction, and, along with the O 1s NEXAFS data (Fig. 3c), suggests a surface layer with more oxygen has been removed.

While the state of the sphere after forming Track #1 is unknown, it is likely that after 3,000 cycles, asperities on the sphere are mechanically removed [17], and a smoother area inside the contact patch, along with chemical passivation, leads to low friction. After making Track #2, the measured final chemical state of the sphere (Fig. 4b) has less C=C and C=O bonded carbon compared with the unworn spectrum, suggesting a surface layer which was removed during sliding. This likely happens during the first $\sim$1,000 passes of high friction. There is some rehybridization of the sp^3-bonded carbon, but the lack of strong C=O or C–H features suggests that either few bonds were broken, or the sp^2-bonded carbon at the surface suffered from wear and the newly exposed surface had a similar chemical makeup. This is a direct result of smoothing the contact area of the sphere, and then passivating any dangling bonds on the sphere with dissociated water.

In both the unworn or worn spectra, there is a noticeable presence of graphitic carbon on the sphere, shown by the higher energy shift of the C=C π^* peak, and the features around 292.0 eV. Previous study showed a hypothetical spectrum that combined HOPG with UNCD [3]. The NEXAFS data from the sphere look similar to this hypothetical spectrum, further supporting that there is a component of graphitic carbon present. If the surface of the unmodified sphere was representative of the bulk, the changes to the chemistry would only be reflected by an increase in the amount of oxygen and C=C bonding. However, the post-wear spectrum has the same line shape as that of the unworn spectrum, except lower features in the pre-edge. It is possible that there is a surface layer that is more oxidized and is removed during mechanical wear.

It is possible that the spectral differences from the as-grown flat and sphere are simply from different coating properties due to the different substrate geometries. The samples, which are placed on a heating stage in the plasma reactor, are all coated in the same run, but the shape of the two substrates means there are different thermal gradients, and possibly different interactions with the plasma. Beyond geometry, the average growth temperature was likely different. The thermal conductivity of Si_3N_4 (0.3 W cm^{-1} K^{-1}) is more than four times less than Si (1.3 W cm^{-1} K^{-1}). This may explain why the coatings of the two surfaces are not identical.

5 Conclusions

Use of a new, laterally resolved NEXAFS technique enabled chemical imaging of both counterfaces of a self-mated sphere-on-flat UNCD contact, specifically, the first time for the sphere surface. Wear tracks, 500 μm in length, were made. The tribometry and interferometry results show that conditioning the UNCD coated sphere leads to faster run-in, lower friction, and lower wear, and does it without graphitizing the flat or sphere. The spectroscopy shows that there is less modification of the flat's surface chemical state when there is lower friction and lower wear. Both the sphere and the flat show evidence of a surface layer that was removed by mechanical wear. Though the sphere started (and ended) with a noticeable presence of graphitic carbon, this alone was not enough to give low friction. Only after some asperity wear during run-in did the system achieve low friction. The newly

conditioned sphere then ran in immediately on a new portion of the flat. It is possible that conditioning either of the counterfaces (sphere or flat) will reduce run-in time. The other possibility is that the sphere is the limiting factor, and needs to be smooth and chemically passivated to reduce the amount run-in. Since a sphere's geometry is changing more rapidly during initial wear, having a non-uniform cross section, it is likely that the sphere is the determining counterface.

While it is unlikely that the chemical state of the sphere after Track #1 was significantly different than after Track #2, this is not known for certain. A more complete study would be to measure the NEXAFS signal after each stage of wear. Removing the sphere between track creation makes it impossible to guarantee that the second track will be created with the same worn region as the first track. Due to these equipment concerns and overall feasibility, the best compromise would be to use identical spheres and have one sphere only undergo run-in, while the other sphere runs in and then creates a second, conditioned track. Examining the final state of each sphere would confirm if the chemistries are similar.

This new imaging tool will open up further avenues for studying tribological problems. Few examples exist of spatially-resolved NEXAFS data from a non-flat tribological counterface [11]. This can be extremely useful for many systems. For example, in the case where the counterfaces are of the same material, but there is a question of whether, due to geometry or exposure, one surface might be changing in a different manner than the other. Also, for systems comprised of different materials, there are questions about material transfer. This new spatially-resolved technique has the ability to answer many questions about chemical composition and bonding of tribological counterfaces.

Acknowledgments Funding was provided by Air Force grant FA9550-08-1-0024. This study was partially supported by the Nano/Bio Interface Center through the National Science Foundation NSEC DMR08-32802. Use of the Center for Nanoscale Materials was supported by the U.S. Department of Energy, Office of Science, Office of Basic Energy Sciences, under Contract No. DE-AC02-06CH11357. Use of the NSLS, Brookhaven National Laboratory, was supported by the U.S. Department of Energy, Office of Science, Office of Basic Energy Sciences, under Contract No. DE-AC02-98CH10886. The LARIAT was developed by Synchrotron Research, Inc. under NIST SBIR funding/Contract No. SB1341-04-C-0021. Certain commercial names are mentioned in this manuscript for purpose of example; this does not constitute an endorsement by the National Institute of Standards and Technology. The authors thank E. Principe for a critical reading of the manuscript. The authors gratefully acknowledge Dr. A.V. Sumant for coating flats and spheres with UNCD.

References

1. Espinosa, H.D., Peng, B., Prorok, B.C., Moldovan, N., Auciello, O., Carlisle, J.A., Gruen, D.M., Mancini, D.C.: Fracture strength of ultrananocrystalline diamond thin films-Identification of weibull parameters. J. Appl. Phys. **94**, 6076–6084 (2003)
2. Espinosa, H.D., Prorok, B.C., Peng, B., Kim, K.H., Moldovan, N., Auciello, O., Carlisle, J.A., Gruen, D.M., Mancini, D.C.: Mechanical properties of ultrananocrystalline diamond thin films relevant to MEMS/NEMS devices. Exp. Mech. **43**, 256–268 (2003)
3. Konicek, A.R., Grierson, D.S., Gilbert, P.U.P.A., Sawyer, W.G., Sumant, A.V., Carpick, R.W.: Origin of ultralow friction and wear in ultrananocrystalline diamond. Phys. Rev. Lett. **100**, 235502 (2008)
4. Hamilton, M. A., Konicek, A. R., Grierson, D. S., Sumant, A. V., Auciello, O., Sawyer, W. G.,Carpick, R. W.: Environmental performance limits of ultrananocrystalline diamond films. In: Proceedings of the STLE/ASME International Joint Tribology Conference, vols. 9–10 (2009)
5. Auciello, O., et al.: Are diamonds a MEMS' best friend? IEEE. Microw. Mag. **8**, 61–75 (2007)
6. Sumant, A.V., Grierson, D.S., Gerbi, J.E., Birrell, J., Lanke, U.D., Auciello, O., Carlisle, J.A., Carpick, R.W.: Toward the ultimate tribological interface: surface chemistry and nanotribology of ultrananocrystalline diamond. Adv. Mater. **17**, 1039–1045 (2005)
7. Sumant, A.V., Grierson, D.S., Gerbi, J.E., Carlisle, J.A., Auciello, O., Carpick, R.W.: Surface chemistry and bonding configuration of ultrananocrystalline diamond surfaces and their effects on nanotribological properties. Phys. Rev. B **76**, 235429 (2007)
8. Kim, H.I., Lince, J.R., Eryilmaz, O.L., Erdemir, A.: Environmental effects on the friction of hydrogenated DLC films. Tribol. Lett. **21**, 53–58 (2006)
9. Eryilmaz, O.L., Erdemir, A.: On the hydrogen lubrication mechanism(s) of DLC films: an imaging TOF–SIMS study. Surf. Coat. Technol. **203**, 750–755 (2008)
10. Chromik, R.R., Winfrey, A.L., Luning, J., Nemanich, R.J., Wahl, K.J.: Run-in behavior of nanocrystalline diamond coatings studied by in situ tribometry. Wear **265**, 477–489 (2008)
11. Anders, S., Stammler, T., Fong, W., Bogy, D.B., Bhatia, C.S., Stohr, J.: Investigation of slider surfaces after wear using photoemission electron microscopy. J. Vac. Sci. Technol. A **17**, 2731–2736 (1999)
12. Anders, S., Stammler, T., Fong, W., Chen, C.-Y., Bogy, D.B., Bhatia, C.S., Stohr, J.: Study of tribochemical processes on hard disks using photoemission electron microscopy. J. Tribol-Trans. ASME. **121**, 961–967 (1999)
13. Canning, G.W., Fuller, M.L.S., Bancroft, G.M., Kasrai, M., Cutler, J.N., De Stasio, G., Gilbert, B.: Spectromicroscopy of tribological films from engine oil additives. Part I. Films from ZDDP's. Tribol. Lett. **6**, 159–169 (1999)
14. Grierson, D.S., et al.: Tribochemistry and material transfer for the ultrananocrystalline diamond-silicon nitride interface revealed by X-ray photoelectron emission spectromicroscopy. J. Vac. Sci. Technol. B **25**, 1700–1705 (2007)
15. Sumant, A.V., Auciello, O., Yuan, H.C., Ma, Z., Carpick, R.W., Mancini, D.C.: Large-area low-temperature ultrananocrystalline diamond (UNCD) films and integration with CMOS devices for monolithically integrated diamond MEMS/NEMS-CMOS systems. Proc. SPIE-Int. Soc. Opt. Eng. **7318**, 731817 (2009)
16. Rennie, A.C., Dickrell, P.L., Sawyer, W.G.: Friction coefficient of soft contact lenses: measurements and modeling. Tribol. Lett. **18**, 499–504 (2005)
17. Hayward, I.P., Singer, I.L., Seitzman, L.E.: Effect of roughness on the friction of diamond on CVD diamond coatings. Wear **157**, 215–227 (1992)
18. Gago, R., Vinnichenko, M., Jager, H.U., Belov, A.Y., Jimenez, I., Huang, N., Sun, H., Maitz, M.F.: Evolution of *sp*2 networks with substrate temperature in amorphous carbon films: experiment and theory. Phys. Rev. B **72**, 14120–14121 (2005)

19. Gago, R., Jimenez, I., Albella, J.M.: Detecting with X-ray absorption spectroscopy the modifications of the bonding structure of graphitic carbon by amorphisation, hydrogenation and nitrogenation. Surf. Sci. **482–485**, 530–536 (2001)
20. Osswald, S., Yushin, G., Mochalin, V., Kucheyev, S.O., Gogotsi, Y.: Control of *sp*2/*sp*3 carbon ratio and surface chemistry of nanodiamond powders by selective oxidation in air. J. Am. Chem. Soc. **128**, 11635–11642 (2006)
21. Coffman, F.L., Cao, R., Pianetta, P.A., Kapoor, S., Kelly, M., Terminello, L.J.: Near-edge X-ray absorption of carbon materials for determining bond hybridization in mixed sp^2/sp^3 bonded materials. Appl. Phys. Lett. **69**, 568–570 (1996)
22. Stohr, J.: NEXAFS Spectroscopy. Springer-Verlag, Berlin (1992)
23. Jaouen, M., Tourillon, G., Delafond, J., Junqua, N., Hug, G.: A NEXAFS characterization of ion-beam-assisted carbon-sputtered thin films. Diam. Relat. Mater. **4**, 200–206 (1995)
24. Ishii, I., Hitchcock, A.P.: The oscillator strengths for C1 s and O1 s excitation of some saturated and unsaturated organic alcohols, acids and esters. J. Electron. Spectrosc. **46**, 55–84 (1988)